Theoretical Analysis of a Dripping Faucet

Bala Ambravaneswaran, Scott D. Phillips, and Osman A. Basaran*
School of Chemical Engineering, Purdue University, West Lafayette, Indiana 47907-1283
(Received 26 January 2000; revised manuscript received 26 May 2000)

While previous studies of continuous emission of drops from a faucet have shown the richness of the system's nonlinear response, a theory of dripping has heretofore been lacking. Long-time behavior of dripping is simulated computationally by tracking the formation of up to several hundred drops in a sequence, rather than the usual single drop, at a given flow rate Q and verified by experiments. As Q increases, the system evolves from a period-1 system through a number of period doubling (halving) bifurcations as dripping ultimately gives way to jetting. That hysteresis can occur is also demonstrated.

PACS numbers: 47.55.Dz, 47.20.Ky, 47.20.Ma, 47.52.+j

Drop formation from a faucet is a ubiquitous phenomenon. It finds applications in areas as diverse as ink-jet printing [1], biochip arrayers [2], and separations [3]. Most studies of drop formation to date have focused on details of drop breakup, examples of which include stability analyses of jets [4], high-speed visualization studies of drop breakup [5,6], and theoretical [7–10] and experimental [8–11] investigations of details of pinch-off. Although the formation of a single drop has received considerable attention for over a century, the parallel problem of the formation of several drops in a sequence—dripping—has been a topic of investigation only in the last decade [12–15]. Following Rössler's [16] suggestion, Shaw [12] carried out a pioneering study on the formation of thousands of drops in succession. The fact that such a simple system, which is found in every household, can exhibit such rich nonlinear dynamics is indeed remarkable. Here, we present an *ab initio* computational analysis of a dripping faucet, which has heretofore defied theoretical analysis, and support the predictions by experiment.

Beginning with Shaw's work [12], all experimental studies of dripping have relied on the use of a drop-counter apparatus wherein a laser beam directed at a detector is interrupted whenever a drop falling from a faucet (tube) crosses the beam's path. Thus the experiment provides the time interval between the drops, $t_1, t_2, \ldots, t_i, \ldots$, where t_i is the time interval between the ith and $(i-1)$th drops. Such studies, however, neglect entirely the physics of drop formation and view the system as a black box that generates a stream of numbers $t_1, t_2, \ldots$. This discretization of the continuous system, which is effected by looking only at $\{t_i\}$, approximates a Poincaré section of the flow in the system state space. A convenient way of analyzing such time interval data to detect possible determinism is by means of time return maps [12,13]. Each point in such a map is determined by the ordered pair (t_n, t_{n+1}) for some n. Previous researchers [12–15] have inferred several structures and patterns from such simple maps indicating that the presumably infinite-dimensional system behaves in a "low-dimensional" fashion. This characteristic of the system has triggered a parallel set of investigations [12,15,17,18] that use simple spring-mass models to surmise the complicated yet low-dimensional behavior of the leaky faucet. Common to these models is the *ad hoc* manner in which drop breakup is mimicked by the removal of a specified amount of mass from the existing mass when the spring extension exceeds a threshold.

Several features distinguish this study from others. Two new approaches, both of which supersede measurement of time intervals, are used to probe the physics of dripping. First, for the first time, the equations that govern the dynamics of Newtonian liquids are solved to predict the formation of hundreds of drops in a sequence from a capillary into air. This computationally intensive task is made possible by the use of a one-dimensional (1D) model based on a slender-jet approximation of the axisymmetric Navier-Stokes equations (ANS) [7,19,20]. In dimensionless form, the 1D equations are

$$\frac{\partial v_z}{\partial t} = -v_z \frac{\partial v_z}{\partial z} - \frac{\partial (2\mathcal{H})}{\partial z} + 3\mathrm{Oh}\,\frac{1}{h^2}\,\frac{\partial}{\partial z}\left(h^2 \frac{\partial v_z}{\partial z}\right) + G\,, \tag{1}$$

$$\frac{\partial h}{\partial t} = -v_z \frac{\partial h}{\partial z} - \frac{1}{2}\, h\, \frac{\partial v_z}{\partial z}\,, \tag{2}$$

where t is time, $h(z,t)$ is the radius of the liquid neck at a distance z from the capillary exit, $v_z(z,t)$ is the axial velocity of the liquid, and $2\mathcal{H}$ is twice the mean curvature. In Eqs. (1) and (2), length and time are measured in units of the capillary radius R and the capillary time $\tau_c \equiv \sqrt{\rho R^3/\sigma}$, respectively, where ρ is the density of the liquid and σ is the surface tension of the liquid-gas interface. The governing dimensionless groups that arise from this formulation are the Ohnesorge number $\mathrm{Oh} \equiv \mu/\sqrt{\rho R \sigma}$, the gravitational Bond number $G \equiv \rho g R^2/\sigma$, and the Weber number $\mathrm{We} \equiv \rho U_f^2 R/\sigma$, where μ is the viscosity of the liquid, g is acceleration due to gravity, and U_f is the average velocity of the liquid in the capillary, related to the flow rate Q by $Q = \pi R^2 U_f$. (The Weber number enters the problem through the imposition of a plug flow velocity profile at the tube exit. Although the actual inflow boundary

 0031-9007/00/85(25)/5332(4)$15.00

condition is parabolic and should be imposed upstream of the tube exit, Ref. [21] shows that this has an insignificant effect on the dynamics.)

The finite element method is used to solve Eqs. (1) and (2), details of which can be found elsewhere [21]. Computations are carried out by starting from an initial state which is, unless otherwise mentioned, a static hemisphere and continued until a specified number of drops are formed. Pinch-off occurs when the dimensionless minimum radius of the fluid neck, h_m, falls below 10^{-3}. It was ensured that the dynamics were insensitive to values of $h_m < 10^{-3}$. Once breakup is detected, the drop that just detached is discarded and a new mesh is constructed. An earlier study [21] has compared predictions made with the 1D model with those made by solving the ANS [10] and shown that for We $\approx \mathcal{O}(0.1)$ the two approaches agree within a few percent so long as $0.01 \lesssim \mathrm{Oh} \lesssim 0.5$, whereas for We $\gtrsim \mathcal{O}(1)$ discrepancies between them become prevalent.

Second, a Kodak Ektapro intensified imager, at rates up to 12 000 frames per second, is used to visualize the entire dynamics of dripping and to verify the computations. In the new experiments, a Sage MP362 syringe pump is used to drive the flow at a constant rate with $\pm 1\%$ accuracy, as opposed to driving it by a constant hydrostatic pressure head as in previous studies [12–14]. It has been ensured by direct observation in the experiments that the contact line remains pinned to the outer sharp edge of the capillary wall throughout the dynamics, as assumed in the computations [21].

At the incipience of breakup, a nearly spherical mass of liquid—a primary drop—is connected via a thin filament—a neck—to a mass of liquid attached to the capillary. Drop formation at low flow rates, or low We, is accompanied by satellite formation due to secondary breakup after the primary drop is formed. The extended neck recoils upward from the point of breakup and pinches off again at its top leading to the formation of the satellite [9,21]. However, as We is increased, previous studies [21,22] have shown that above a critical We $\equiv$ We$_c$ there is insufficient time for the secondary pinch-off to occur before the next primary drop forms. Here, attention is focused on situations in which We $>$ We$_c$ so that satellites are not formed.

For We $\gtrsim$ We$_c$, the system exhibits a period-1 response where the dynamics is the same from one drop to the next. In this case, $t_{n+1} = t_n$ and the time return map is just a single point on the diagonal line in (t_{n+1}, t_n) space. Figure 1(a) shows an example of such a period-1 response for a system characterized by Oh $= 0.1$ and $G = 0.5$, henceforward referred to as system S, at We $= 0.12$. The evolution with We of the dynamics of this system will be discussed in detail in this paper. Figure 1 also shows time return maps for this system, (b) and (c), and another system, (d), when We > 0.12. These will be referred to throughout the paper in order to highlight various nonlinear responses.

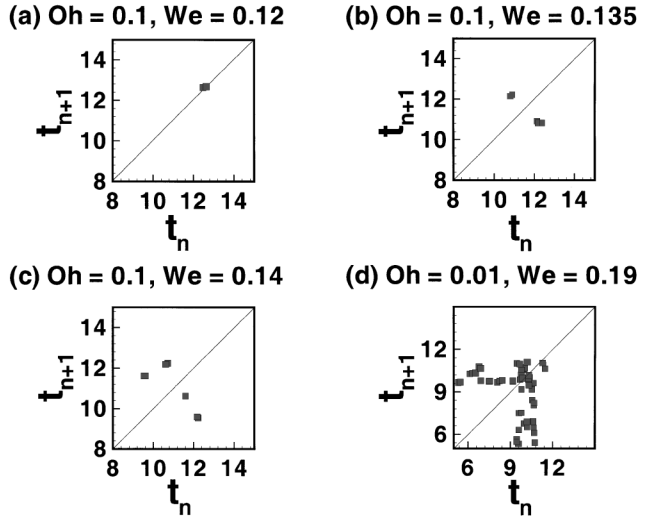

FIG. 1. Time return maps of responses that are (a) period-1, (b) period-2, (c) period-4, and (d) chaotic. Here $G = 0.5$. In (a)–(c), Oh $= 0.1$ and We $= 0.12$, 0.135, and 0.14. In (d), Oh $= 0.01$ and We $= 0.19$.

A convenient way of displaying the response of system S to changes in We is by the bifurcation diagram of Fig. 2. This diagram shows the variation of the dimensionless lengths of drops at breakup, L_d, henceforth termed limiting lengths, with We. In the period-1 regime as seen from Fig. 2 for We $\lesssim 0.125$, there exists only one limiting length corresponding to each value of We. As the flow rate is increased, system S undergoes a period doubling bifurcation at We ≈ 0.125 resulting in a period-2

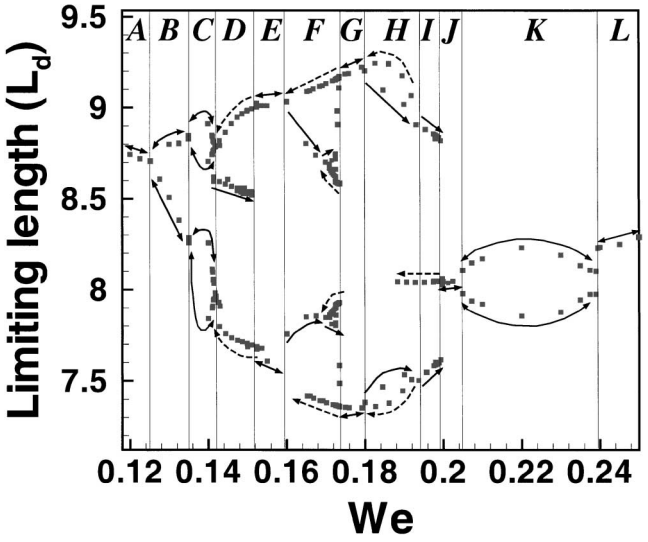

FIG. 2. Bifurcation diagram for a system characterized by Oh $= 0.1$ and $G = 0.5$ with We as the bifurcation parameter and L_d as the response. The We range is divided into zones of different responses. Zone A: period-1; zone B: period-2; zone C: period-4; zone D: hysteresis between period-1 and period-2 paths; zone E: period-2, zone F: parallel hysteresis between several period-2 paths; zone G: period-2; zone H: parallel hysteresis between a period-1 and two period-2 paths; zone I: hysteresis between period-1 and period-2 paths; zone J: period-1; zone K: period-2; and zone L: period-1.

system where every other drop is formed in an identical fashion. This bifurcation is made plain in Fig. 2, e.g., at We ≈ 0.135, where the existence of two limiting lengths at a given value of We can clearly be seen. The corresponding time return map in this period-2 regime is shown in Fig. 1(b). This map consists of points corresponding to over 50 consecutively formed drops and the period-2 response is made evident by the clustering of data around two points, viz. $t_{n+2} = t_n$.

Figure 3 compares experimentally observed (top row) and computationally predicted (bottom row) shapes at breakup of ten successive drops in such a period-2 regime for a system consisting of a 70% glycerin in water solution dripping from a capillary of $R = 0.15$ cm when $Q = 40$ mL/min (Oh $= 0.069$, $G = 0.43$, and We $= 0.26$). Although period doubling in a dripping faucet has been inferred by several experimentalists from time interval data, this is the first time that it has been determined by computation or direct visualization. The values of L_d for the long and short drops were, respectively, 8.6 and 7.0 in the experiments and equaled 8.4 and 7.2 in the computations. The measured values of the long and short time intervals were, respectively, 91 ms and 54 ms while the computed values equaled 88 ms and 51 ms. For this system characterized by Oh $= 0.069$ and $G = 0.43$, the onset of period-2 response occurred when We ≈ 0.223 in the experiments and We ≈ 0.226 in the computations. The remarkable agreement found between experimental and computational results reported in this paragraph and in other situations (not shown) justifies the use of the 1D model to study the formation of hundreds of drops in a sequence. More reassuringly, computed values of L_d and drop volume(s) remain unchanged to five or six decimal places after as many as 100 periods even in the vicinity of bifurcation points.

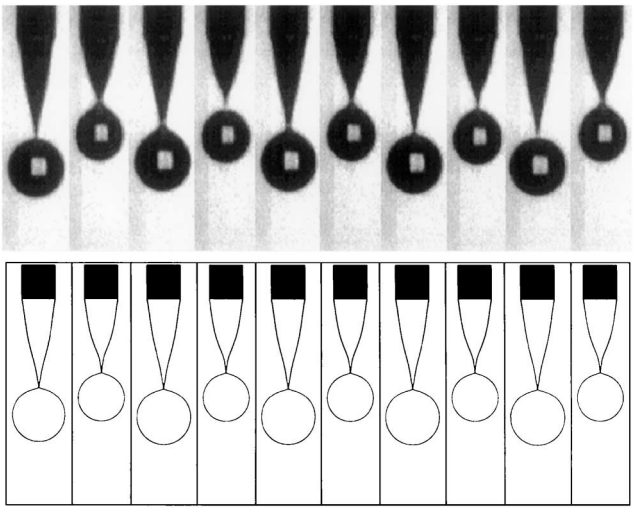

FIG. 3. Experimental observation (top row) and computational prediction (bottom row) of period-2 response of a system characterized by Oh $= 0.069$ and $G = 0.43$ when We $= 0.26$. These shapes are of ten consecutive drops after initial transients have died out and period-2 response has set in.

System S exhibits a plethora of interesting behavior as We increases. To emphasize the different responses that are observed as We is varied, Fig. 2 is divided into several zones. The types and directions of the arrows shown in Fig. 2 and Fig. 4 to follow are clarified below. Thus, zone A represents the period-1 regime which bifurcates into the period-2 regime referred to as zone B. System S undergoes yet another period doubling bifurcation to yield a period-4 response, where every fourth drop is formed in an identical fashion, viz. $t_{n+4} = t_n$, as zone B gives way to zone C. This characteristic is clearly seen from the bifurcation diagram in Fig. 2, which shows that there are four different limiting lengths at the same values of We in zone C, e.g., at We ≈ 0.14, and also from the time return map shown in Fig. 1(c). Further increases in We result in a bifurcation that causes the system to revert back to period-2 response near the end of zone C, as shown in Fig. 2.

Most interestingly, a sudden transition takes place from a period-2 response at the end of zone C to a period-1 response at the beginning of zone D. Thereafter the system follows the path indicated by the solid single-headed arrow as We is increased. This transition is the result of a sudden jump and differs from the bifurcation from a period-4 to a period-2 response that is seen in zone C. This sudden jump indicates the possibility of hysteresis where the dynamics may follow a different path were We to be decreased. To test this hypothesis, the numerical algorithm has been modified to compute steady dripping at a Weber number We $\pm$ ΔWe, where ΔWe is a small increment, by using the solution at We as the initial condition. These runs, referred to as sweeps, differ from those discussed so far. Such sweeps revealed that the system jumps again, but now from a period-1 response in zone D to a period-2

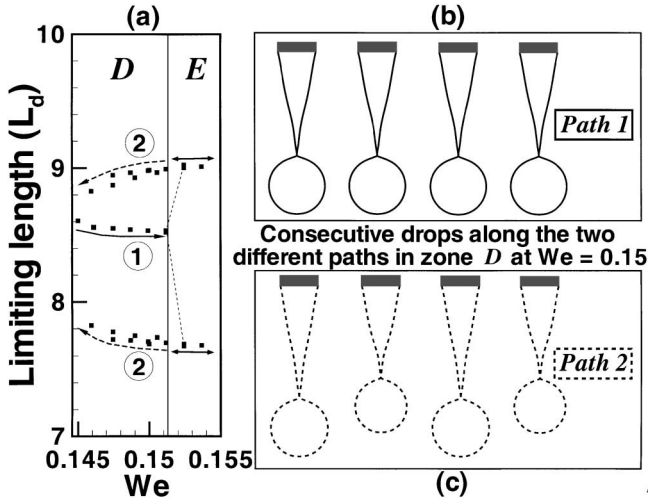

FIG. 4. Close-up of zones D and E of Fig. 2, (a), and sequence of shapes of drops at breakup obtained at We $= 0.15$ when following different hysteresis paths, (b) and (c). Here path 1, (b), exhibits a period-1 response and is encountered when We is increased while path 2, (c), exhibits a period-2 response and is encountered when We is decreased. The dashed lines in (a) indicate a jump from the end of path 1 to path 2.

response in zone E as We is increased. Once in zone E, if We is decreased in a sweep mode then the dynamics follow a path into zone D that is entirely different from the path encountered in zone D when We is increased. Not too surprisingly, the new path followed, indicated in zone D by the dashed single-headed arrows, reaches the original period-2 system that has already been seen at the end of zone C. To emphasize the path dependence of solutions, in Figs. 2 and 4 solid double-headed arrows indicate paths that are followed uniquely, whereas solid and dashed single-headed arrows indicate paths followed whenever We is increased and decreased, respectively.

Figure 4 shows a close-up of the bifurcation diagram of Fig. 2 to emphasize the occurrence of hysteresis in zone D. Two distinct paths that the dynamics follow when We is increased and decreased in a sweep mode are labeled 1 and 2, respectively. In Figs. 2 and 4, it should be noted that at a given value of We solid double-headed arrows indicate that the system sees all the limiting lengths corresponding to that particular We. By contrast, single-headed arrows indicate that the system exists in either one of the states and follows either one of the paths, but not both, indicated by the arrows. Thus Fig. 4 shows that at a particular We in zone D, the response is period-1 if We is increasing whereas it is period-2 if We is decreasing. Figure 4 shows the dramatically different shapes of four consecutive drops along each of these paths when We $= 0.15$. Thus either the sequence of drops shown by solid lines [Fig. 4(b)] or the sequence of drops shown by dashed lines [Fig. 4(c)], but not both, may be observed when We $= 0.15$.

Figure 2 shows several other zones where hysteresis occurs. Zones A, B, C, E, G, J, K, and L are those in which the paths followed by the dynamics are unique for each We encountered in them; i.e., hysteresis is absent in these zones. In zone I a response opposite to that encountered in zone D is obtained; i.e., the response is period-2 for increasing We and is period-1 for decreasing We. Zones F and H differ from others in that there are two different paths for the drops to follow when We is decreased in a sweep mode. In zone F, there is a small hysteresis loop consisting of two distinct period-2 responses. In zone H, the system may exhibit either a period-1 or a period-2 response as We is decreased depending on the line of approach. Zone J shows the return to a simple dripping regime with period-1 response, while zone K results from a period doubling bifurcation from zone J. From Fig. 2 it can be noted that the response of the system returns to period-1 when We $\gtrsim 0.24$ in zone L. System S jets when We $\gtrsim 0.26$.

According to the foregoing results, dripping from a leaky faucet can exhibit fascinating behavior ranging from expected to unexpected. It has been shown here for the first time experimentally or theoretically that hysteresis can occur in a dripping faucet. Using time interval data, previous studies have demonstrated that several routes to chaos exist in a dripping faucet [23]. Figure 1(d) shows a time return map, predicted by the 1D model, that resembles a strange attractor. This map corresponds to a system less viscous than system S, such that Oh $= 0.01$ and $G = 0.5$ when We $= 0.19$. By contrast, no chaotic regimes have been found for system S. Ongoing work in our laboratory [24] has shown that when Oh $\approx \mathcal{O}(1)$, the system transitions directly from period-1 response to jetting as We increases.

This research was sponsored by the Chemical Sciences Program of the BES Division of the U.S. DOE and a research grant from Eastman Kodak.

*Electronic address: obasaran@ecn.purdue.edu

[1] I. Rezanka and R. Eschbach, *Recent Progress in Ink Jet Technologies* (IST Press, Springfield, VA, 1996).
[2] R. Pappen, in *Proceedings of the IBC International Conference on Massively Parallel DNA Analysis, San Francisco, CA, 1998* (International Business Communications, Southborough, MA, 1998).
[3] W. J. Heideger and M. W. Wright, AIChE J. **32**, 1372 (1986).
[4] Lord Rayleigh, Proc. London Math Soc. **10**, 4 (1879).
[5] H. E. Edgerton, E. A. Hauser, and W. B. Tucker, J. Phys. Chem. **41**, 1017 (1937).
[6] D. H. Peregrine, G. Shoker, and A. Symon, J. Fluid Mech. **212**, 25 (1990).
[7] J. Eggers and T. F. Dupont, J. Fluid Mech. **262**, 205 (1994).
[8] X. D. Shi, M. P. Brenner, and S. R. Nagel, Science **265**, 219 (1994).
[9] M. P. Brenner *et al.,* Phys. Fluids **9**, 1573 (1997).
[10] E. D. Wilkes, S. D. Phillips, and O. A. Basaran, Phys. Fluids **11**, 3577 (1999).
[11] D. M. Henderson, W. G. Pritchard, and L. B. Smolka, Phys. Fluids **9**, 3188 (1997).
[12] R. Shaw, *The Dripping Faucet as a Model Chaotic System,* The Science Frontier Express Series (Aerial Press, Inc., Santa Cruz, 1984).
[13] P. Martien, S. C. Pope, P. L. Scott, and R. S. Shaw, Phys. Lett. **110A**, 399 (1985).
[14] X. Wu and Z. A. Schelly, Physica (Amsterdam) **40D**, 433 (1989).
[15] A. D'Innocenzo and L. Renna, Int. J. Theor. Phys. **35**, 941 (1996).
[16] O. Rössler, in *Synergetics: A Workshop: Proceedings of the International Workshop on Synergetics at Schloss Elmau, Bavaria, 1977,* edited by H. Haken (Springer-Verlag, New York, 1977).
[17] G. I. Sánchez-Ortiz and A. L. Salas-Brito, Physica (Amsterdam) **89D**, 151 (1995).
[18] A. Tufaile *et al.,* Phys. Lett. A **255**, 58 (1999).
[19] M. A. Matovich and J. R. A. Pearson, Ind. Eng. Chem. Fund. **8**, 512 (1969).
[20] A. L. Yarin *et al.,* Phys. Fluids **11**, 3201 (1999).
[21] B. Ambravaneswaran, E. D. Wilkes, and O. A. Basaran (to be published).
[22] X. Zhang, J. Colloid Interface Sci. **212**, 107 (1999).
[23] K. Dreyer and F. R. Hickey, Am. J. Phys. **59**, 619 (1991).
[24] B. Ambravaneswaran, S. D. Phillips, and O. A. Basaran (to be published).